Journal Pre-proof

Simultaneous adsorption of quinoline and dibenzothiophene over Ni-based mesoporous materials at different Si/Al ratio

L. Alvarado-Perea, J.A. Colín-Luna, A. López-Gaona, Tanya Wolff, J.G. Pacheco-Sosa, J.C. García-Martínez

Simultaneous adsorption of quinoline and dibenzothiophene over Ni-based mesoporous materials at different Si/Al ratio

L. Alvarado-Perea [a], J. A. Colín-Luna [b], A. López-Gaona [c], Tanya Wolff [d], J. G. Pacheco-Sosa [e], J. C. García-Martínez [b] [*]

[a] Universidad Autónoma de Zacatecas, Unidad Académica de Ciencias Químicas y Maestría en Ciencias de la Ingeniería, Campus UAZ Siglo XXI, Carretera Zacatecas-Guadalajara km 6, Ejido La Escondida, CP. 98160, Zacatecas, México.

[b] Universidad Autónoma Metropolitana Azcapotzalco, Departamento de Energía, Área de Análisis de Procesos, Av. San Pablo 180, Col. Reynosa, CP. 02200, México, CDMX.

[c] Universidad Autónoma Metropolitana Iztapalapa, Departamento de Química, Av. San Rafael Atlixco 186, Col. Vicentina, CP. 09340, México, CDMX.

[d] Max Planck Institute for Dynamics of Complex Technical Systems, Sandtorstr. 1, 39106 Magdeburg, Germany

[e] Universidad Juárez Autónoma de Tabasco (UJAT), División Académica de Ciencias Básicas, Km 1, Carretera Cunduacán-Jalpa de Méndez, Col. La Esmeralda, CP. 8669, Cunduacán, Tabasco, México.

(*) corresponding author: jgarciam@azc.uam.mx

1

Graphical abstract
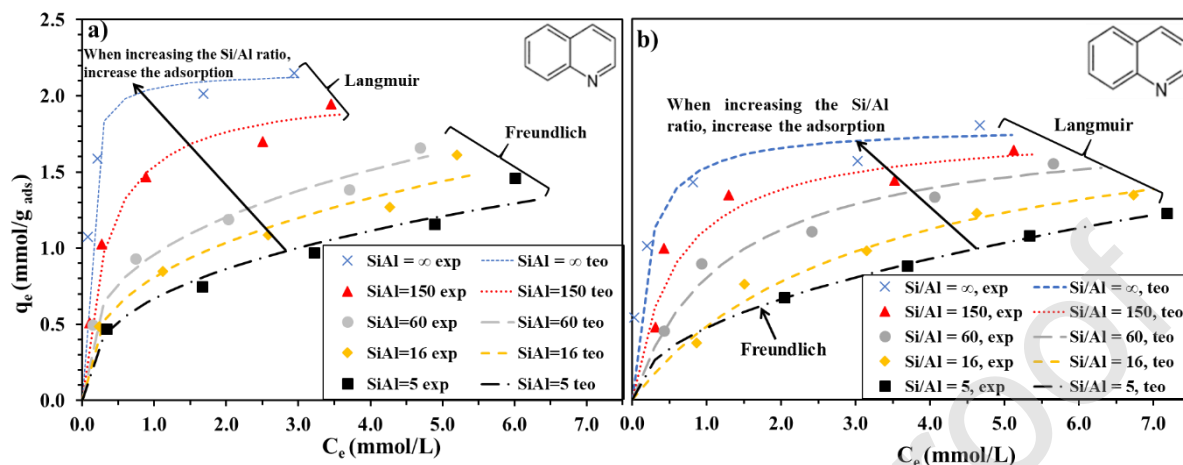
Adsorption isotherms with a) MCM-41 and b) Ni/MCM-41 varying the Si/Al ratio with Q in the presence of DBT, with a ratio S:N=1. Dashed lines represent the Langmuir or Freundlich model.

Highlights

- Q was adsorbed with MCM-41 and Si/Al ratio as 150 and ∞

- With Ni/MCM-41 the sulfur adsorption with Si/Al = 5 is presumably related to the Lewis sites acidity

- Langmuir and Freundlich's isotherm were adjusted for N adsorption and MCM-41 presenting higher values of adsorption processes

- Freundlich isotherm was adjusted for sulfur adsorption and it was the best model for both adsorbents

Abstract

In this study, two mesoporous materials such as MCM-41 and Ni/MCM-41 were modified with Al at different Si/Al ratios. The mesoporous materials were proved as sorbents of heterocyclic nitrogen and sulfur compounds employing quinoline (Q) and dibenzothiophene (DBT), respectively, as model molecules of that precursor pollutants at the same concentrations of ppmw of nitrogen and sulfur (N:S = 1 ratio). The sample with the highest Si/Al ratio showed the highest specific surface, and at low Si/Al decreased the specific surface. With X-ray diffraction (XRD) the Ni containing in MCM-41, there is a clear trend and the highly hexagonal ordered sample is the one without Al and once the Al is added, the hexagonal ordering is highly modified. Employing NH_3-TPD and NMR revealed that the samples with Si/Al = 5 and 16 have higher Lewis acid sites than another ratio of Si/Al. The modification successfully added small amounts of Ni that did not collapse the pore structure but increased the density of surface (acidic) groups that in turn favored the uptake of the sulfur compound through π-complexation adsorption mechanism. It is also possible to recognize that the samples with a Si/Al ratio of 5 and 16 revealed the presence of the highest surface density of weak acid sites for both sorbents. Adsorption experiments were carried out in a batch adsorption system at 313 K and atmospheric pressure using a model mixture from diesel containing: DBT, Q, and 40 ml of dodecane. The sulfur adsorption was substantially improved when Ni was incorporated to MCM-41; for example, at 250 ppmw of N uptake of DBT was almost twice than MCM-41 alone. This result would indicate that Ni/MCM-41 could remove both molecules but mainly the nitrogen molecule at high concentrations. The Langmuir and Freundlich adsorption isotherms were used for all materials considering Q in the presence of DBT depending on the Si/Al ratio. This behavior did not happen for the DBT whose behavior was modelled by an isotherm of the Freundlich type for Ni/MCM-41 and adsorbed in acid sites and multilayer. Lastly, experimental

3

results indicated that MCM-41 with Si/Al = ∞ has the highest (Q/DBT) selectivity of 13,390 at 50

ppmw N compared to another Si/Al ratio, for example, at 250 ppmw N.

1. Introduction

Despite new energy sources (biodiesel, bioethanol, green diesel, and others) less contaminants than fossil fuels [1,2], the world faces the challenge to cover the demand for automotive fuels that could not be reached only with fuels from biomass [2]. This has led to the refiners to improve their processes to achieve high production of gasoline and diesel, taking care of the rigorous environmental regulations regarding the sulfur content (<10 ppm) in diesel fuels. The typical process to reach low sulfur levels is through the hydrodesulfurization (HDS) reaction, employing a sulfured catalyst usually Co-MoS or Ni-MoS supported on alumina at severe conditions of temperatures (> 573 K) and hydrogen pressures (> 5.5 MPa) [3]. The severe-operating conditions, high hydrogen consumption and considering that organo nitrogenated molecules contained in the diesel cuts deactivate the catalyst, making the process unaffordable.

An alternative process to reach the stringent environmental legislation regarding sulfur content, is using adsorption of organo-compounds employing functionalized mesoporous materials before HDS [4-7]. This kind of process has the advantage of being carried out at temperatures below of 353 K, atmospheric pressure and does not require hydrogen consumption. The crucial part of the process is the kind of adsorbent material employed because the adsorption of the sulfur and nitrogenous molecules would depend on the physicochemical and textural properties of the adsorbent [6-8]. Zeolites [5,9-13], activated carbons [14-20], activated alumina, metal oxides, and mixed oxide [8, 21-25] are the most common adsorbents. Although the choice of these materials should be made considering adsorption capacity, selectivity, regenerability, lifetime, and price,

4

some properties must be considered. For instance, activated carbons have shown that not only their high specific area and the highest polarity are the cause of the removal of N-compounds that activated alumina, but also their high oxygen groups density and acidic functional groups. Almarri et al. [15] and Arcibar-Orozco et al. [18] found that carboxyl and carboxylic anhydride groups are acidic functional groups contributed to adsorption of Q, whereas primary basic oxygen-containing groups, such as carbonyl and quinone groups, contributed to adsorption of indole and followed the order in terms of more favorable adsorption: Indole > Q > 4,6-dymethildibenzothiophene (4,6-DMDBT) > DBT. Moreover, the activated carbons have larger surface areas (> 1000 m^2/g) but a microporous network that would limit the adsorption of large sulfur molecules such as dibenzothiophenes or alkyl dibenzothiophenes, like 4,6-DMDBT commonly contained in diesel cuts. Besides, activated carbons can form small particles or fines due to their low mechanical resistance causing high-pressure drops in continuous adsorption processes. These drawbacks restrict their use in industrial processes [4].

Zeolites are reported as adsorbents highly sulfur-selective employed commonly to adsorb sulfur compounds and have pore diameters from microporous order and surface areas lower than (800 m^2/g). There is an extensive broad consensus in the literature, that this high capacity and selectivity towards the sulfur compound is not only due to its acid properties but rather to the incorporation of metals (Cu^{+1}, Ag^{+1}, Fe^{+2}, Zn^{+2}, Cd^{+2}, Mn^{+2} or Ni^{+2}) in the cavities of the zeolite [7, 13]. It has been determined that Cu^{+1} is stronger than Ag^{+1} in the binding with sulfur and that this binding is by π-complexation. In this type of non-covalent interaction, there is a donation of electron charges from the orbital π of the sulfur compound to the vacant s orbital of metals (known as σ donation) and, simultaneously, a back-donation of electron charges from the d orbitals of metals to the orbital π anti-bounding of the sulfur compound [5]. Most of the literature highlight

Cu or Ag on zeolites [12]. Recently, Liao et al. [13] modify de acidic properties NaY zeolite using different concentrations of NH_4NO_3 (0.05-1.0 mol/L) solutions and different calcination temperatures (673 - 1023 K), Lewis acid sites bring on the adsorption of compounds containing conjugated π bond as benzene and thiophene (Ti), whereas Brönsted acid site brings on the Ti are significant to determine the properties to remove sulfur compounds [15]. In the first synthesis, they found an equilibrium in the quantity of Lewis and Brönsted acidic sites, whereas calcination treatment generated Lewis acid sites, principally, due to the substitution of Al trivalent for tetravalent Si in the first treatment, and dehydroxylation in the second one [15]. An opposite effect was found in HY zeolites under calcination, where a decrease in sulfur removal occurred with the calcination temperature.

One possibility to remove sulfur compounds of larger sizes, as described above, is employing mesoporous silica materials with pores size larger than 3 nm and surfaces areas nearby to 1000 m^2/g [23-26]. Recently, our group proved several kinds of mesoporous materials such as SBA-15, SBA-16, and MCM-41 as adsorbents of Q and DBT as model molecules representatives from diesel mixtures at 318 K and atmospheric pressure in a batch system and using different molecules [27,28]. It was postulated that high surface area and Si-OH groups (Brönsted acid sites) at that adsorption temperature, allowed selective adsorption of Q but weak adsorption of the sulfur molecule.

Therefore, in this paper is proposed to prove an MCM-41 modified with Al at several Si/Al ratios (5, 16, 60, 150 and ∞) and incorporating Ni on mesoporous silica in the adsorption of Q as the nitrogen molecule and DBT as a sulfur molecule in a mixture molecule from diesel. The influence of structural, textural, morphology and acidity of materials used was investigated to give a scientific explanation, were used at the same concentration of 50, 100, 150 200 and 250 ppmw

6

and N:S = 1 ratio. A metal effect was shown to improve the adsorption sites of the sulfur molecule and selectivity.

2. Experimental

2.1. Synthesis of MCM-41 and Ni/MCM-41 as adsorbents

In this work, the synthesis of MCM-41 and Ni/MCM-41 with different amount of Al was carried out. These materials were prepared using the procedure reported by Alvarado-Perea et al. [29]. A typical procedure was performed as follows: tetrabutylammonium silicate was prepared with a mixture of 5.4 g of a solution of tetrabutylammonium hydroxide 40 wt.%, and 0.6 g of silica fumed (both from Sigma Aldrich). The latter component was mixed with another solution formed by 3.4 g of cetyltrimethylammonium bromide, CTABr (Merck, CTABr ≥ 97%) and 23.3 g of deionized water. The resultant mixture was stirred for 15 min; at the end, the mixture had a molar composition of 1 SiO_2: 0.35 CTABr: 0.31 TBAOH: 55 H_2O. That mixture was transferred to a Nalgene bottle and aged for 48 h at 373 K. The resultant solid was recovered by vacuum filtration and washed five times with 250 ml of deionized water each time. The final powder was dried at 353 K for 6 h. Finally, the solid obtained was heated up to 873 K in air at a heating rate of 5 K/min and it was kept at this temperature for 6 h. The Ni/MCM-41 was prepared using the template ion exchange method [30]. In a typical essay, 3.0 g of synthesized MCM-41 was mixed with 30 mL of deionized water. To the previous mixture, 30 mL of a solution 0.03 M of Ni^{+2} was added dropwise under vigorous stirring. The Ni precursor was $Ni(NO_3)_2 \cdot 6H_2O \geq 99.0$ % from Merck. The resulting mixture was transferred into a Nalgene bottle and treated at 353 K for 20 h without stirring. The solid was recovered by vacuum filtration, washed with deionized water and dried at 353 K for 24 h. The final product was calcinated at 873 K for 6 h in air and the heating rate was 5 K/min. The characterization of Ni/MCM-41 material was already published and discussed by Alvarado-Perea et al. [29], a brief description is presented below.

2.2. Characterization of MCM-41

2.2.1. Structural Analysis

Powder X-ray diffraction (XRD) patterns were collected on an X'Pert PRO diffractometer by PANalytik using Ni-filtered CuKa radiation. The generator was operated with a voltage of 40 kV

and a current of 40 mA. All samples were scanned in the small 2θ region (1-10º) with a step size of 0.016º using a scanning time of 10 s per step.

2.2.2. Textural analysis

Nitrogen physisorption isotherms were measured at -196 °C using a Quantachrome Nova 2200 e analyzer. Specific surface areas were calculated from the linear region of BET plots while the total pore volume was evaluated using the amount adsorbed at a relative pressure of 0.995.

2.2.3. Transmission electron microscopy (TEM)

The morphological TEM analysis was performed by using a Philips/FEI CM200 microscope. The apparatus was operated at an acceleration voltage of 200 kV and equipped with a CCD camera for the imaging acquisition and analySISpro SIS/ Olympus processing system.

2.2.4. Temperature Programmed Desorption of Ammonia (NH₃-TPD)

Surface acidity was investigated by Temperature Programmed Desorption of Ammonia experiments (NH₃-TPD). The samples were pre-treated at 500 ºC in helium for 2 h, followed by cooling to 100 ºC. Ammonia (1 vol.% NH₃ in He) was then adsorbed at the same temperature for 2 h. Physisorbed molecules were removed by switching back to a pure helium flow (also at 100 ºC) for 1 h. Finally, the temperature was raised to 650 ºC with a heating rate of 10°C/ min. Desorbed ammonia was detected with a TCD.

2.2.5. ^{29}Si and ^{27}Al Nuclear Magnetic Resonance (NMR)

NMR spectra were recorded using a Bruker Avance 300 NMR spectrometer at room temperature. The ^{29}Si shifts were externally referenced to Q8M8. The ^{27}Al shifts scales were externally referenced to $[Al (H_2O)_6]^{3+}$.

2.3. Adsorption experiments

Adsorption experiments were performed in jacketed glass containers at atmospheric pressure and 313 K. All adsorbents were crushed and sieved at 100 mesh, the amount of adsorbent was of 0.2 g, it is an optimal amount where there are no problems of mass transfer, external or internal experimentally it was verified. Also, several experiments have been performed and this quantity was determined as optimal, especially to prevent the solid from agglomerating in the liquid [27,28,31]. Adsorptive denitrogenation and desulfurization of model nitrogen and sulfur-containing compounds in dodecane were performed using the following adsorbents: MCM-41 and Ni/MCM-41 in batch mode. The nitrogen and sulfur concentrations were fixed between 0 and 250 ppmw of S and N in 40 mL of dodecane, with N:S=1 ratio. In each experiment, the mixture was stirred at 400 rpm, until complete homogenization, and at that instant (t_0), a sample was collected in a vial for further analysis in a capillary gas chromatograph brand Perkin-Elmer model Clarus 480, equipped with a capillary column (methylphenylsilicone, EC-5 ECONOCAP) and injector and flame ionization detector (FID) 200 and 250 ℃, respectively. To achieve the separation of the organ compounds, two heating ramps were used in the oven. The first, from 160 ° C until 200 ° C for 2 min at a heat rate of 5 K/min and the last one at 250 for 2 min at a heat rate of 20 K/min. The samples were collected every 5 min during the first hour and every 15 min for the next two hours; the sample volume was 0.3 mL. The sampling process represents a reduction of the total volume by only around 10 %. All samples were filtered to avoid introducing the adsorbent to the gas chromatograph. The adsorption capacities of nitrogen and sulfur compounds (AC_S and AC_N, respectively) were obtained, such as described in a previous works [27,28,31].

9

Sulfur and nitrogen removal were calculated through Eq. (1).

$$AC_S \text{ or } AC_N \ (\%) = \frac{(C_0 - C_e)}{C_0} \times 100 \tag{1}$$

Where C_0 and C_e represents the concentration in mmol L^{-1} of sulfur of nitrogen compound at the initial time at the equilibrium, respectively.

Moreover, the selectivity was defined in terms of the ratio of adsorption and equilibrium concentration of N/S ratio, according to Songolzadeh et al. [33], defined like:

$$S = \frac{q_N/q_S}{C_{e,N}/C_{e,S}} \tag{2}$$

2.4. Adsorption kinetics

Regarding the adsorption rate, the literature mentions several models that can be fitted to the experimental data. Azizian and Fallah [32] made a review of these models. To understand the adsorption process, the commonly used kinetic models, the pseudo-second-order model was examined to describe the nitrogen adsorption kinetics of newly developed adsorbents. The pseudo-second-order model assumes that the rate-limiting step of a reaction may be chemisorption, which involves valence forces by electron sharing or electron exchange between the adsorbent and the adsorbate. This equation can be expressed as:

$$r = \frac{dq_t}{dt} = k_{ads}(q_e - q_t)^2 \tag{3}$$

$$\frac{t}{q_t} = \frac{1}{k_{ads}\, q_e^2} + \frac{t}{q_e} \tag{4}$$

where q_t (mmol/g) is the amount adsorbed at each time (min), k_{ads} (g/(mmol min)) is the adsorption rate constant of pseudo-second-order adsorption, and r is the adsorption rate. The slope and intercept of the linear plots of t/q_t against t yield the values of $\frac{1}{q_e}$ and $\frac{1}{k_{ads}\, q_e^2}$. The values of q_e and k_{ads} can be obtained from the slope and intercept.

2.5. Adsorption isotherms

10

The Langmuir isotherm is the most common model used to quantify the amount of adsorbate on the surface of the adsorbent as a function of partial pressure or concentration at a given temperature and occurs on the homogeneous surface with monolayer formation without any interaction. On the other hand, the Freundlich isotherm is an empirical equation employed to describe heterogeneous systems and multilayer adsorption and has been used for heterogeneous surface energy systems with the random distribution of sorption heat, the magnitude of the exponent $1/n$ indicates the variability of adsorption. For example, if $1/n = 1$, the adsorption is linear; this is the Henry's law behavior occurs, meanwhile $1/n > 1$ represent favorable adsorption conditions and $1/n < 1$ an unfavorable adsorption also chemisorption process related to the adsorption capacity of the adsorbents and surface heterogeneity. The parameters of these isotherms were used in the same way by our group [27,28,31]. The results obtained with two adsorbents are presented in the next section.

3. Results and discussion

3.1. Characterization of MCM-41 and Ni/MCM-41

In this section it is presented the results of characterization of the materials used for the adsorption process.

3.1.1. Structural analysis and textural analysis

In this work, the characterization results of the MCM-41 and Ni/MCM-41 materials varying the Si/Al ratio were shown. In this way, the XRD patterns of the MCM-41 and Ni/MCM-41 with different Si/Al ratio are shown in Fig. 1a and Fig. 2a, respectively. As it is well known, MCM-41 materials are characterized by typical diffractions (100), (110), (200) and (210) [34,35]. From the Fig.1a, it is possible to observe that there is not a clear trend of the patterns of the MCM-41 samples at different Al contents. For example, the case of MCM-41-Si/Al = ∞ (without Al) did not show any characteristic peak at any value of 2θ. However, the sample with at Si/Al = 150 revealed the

11

typical diffraction pattern of the MCM-41 materials. For the samples with higher Al content, the typical diffraction patterns of the MCM-41 materials decreased because of the hard incorporation of the Al into the network of the materials. Based on the last results, it is concluded that these materials are poor hexagonal ordered. On the other hand, for the case of the Ni containing MCM-41, (Fig. 2a) we can see that there are a clear trend and the highly hexagonal ordered sample is the one without Al and once the Al is added the hexagonal ordering is highly modified. Besides, it seems that the method of the Ni incorporation improves the ordering of MCM-41 materials [29]. These results it has already been shown by Yonemitsu et al. [30] whose found that the Ni impregnation method rearranges the pore structure of MCM-41. Based only on the XRD results, it is not possible to ensure that the structure of the materials does not correspond to the typical MCM-41 materials. For this reason, all materials were also characterized using N_2-physisorption. Moreover, MCM-41 and Ni/MCM-41 materials are also characterized by a Type IV nitrogen isotherm, pore diameter in the range of mesoporous and by a high specific surface [34,35]. Fig. 1b and Fig. 2b shows the adsorption isotherms and the adsorption data of the MCM-41 and Ni/MCM-4a with different Si/Al ratios, respectively. These results revealed the presence of a type IV isotherm according to IUPAC classification for both adsorbents [36]. It is possible to observe that the N_2 adsorption data do not depend strongly on the Si/Al ratio of the MCM-41. Table 1 shows the results of the MCM-41of BET specific surface, pore-volume and pore diameter, almost all samples presented a specific surface (around 1,000 m^2 g^{-1}), and only the sample with the highest Al content (Si/Al=5) had an important reduction of the specific surface (554 m^2 g^{-1}). An important modification of the pore volume was observed and the sample with a Si/Al ratio of 16 showed the highest value (2.31 cm^3 g^{-1}). This modification might be caused by the high Al content in the materials. Additionally, in the same way than Table 1, the results of Ni/MCM-41 varying the Si/Al are presented in Table 2 we can see that the highest value of specific surface was at Si/Al=150

12

(1,385 m^2 g^{-1}) followed by Si/Al = ∞ (1,087 m^2 g^{-1}) [29], moreover the Ni incorporation into the MCM-41 network revealed just important modifications in the pore volume of the samples. In this case, the sample with a Si/Al ratio of 150 showed the highest value (2.0 cm^3 g^{-1}).

3.1.2. Transmission Electron Microscopy (TEM)

To visualize the arrange and Ni effect on the morphology, TEM micrographs are shown in Fig. 3 for the samples; (a) MCM-41, (b) Ni/MCM-41, (c) Ni/MCM-41 (Si/Al=150) and (d) Ni/MCM-41 (Si/Al=16). In general, almost all adsorbents showed hexagonal pores arrange, which is characteristic of the MCM-41 materials. For the case of the Ni containing samples, it was observed the presence of a mixture of MCM-41 structure and Ni films. For the case of the sample with a Si/Al ratio of 150 it was also observed Ni particles. These particles were not observed for the case of the sample with a Si/Al ratio of 16. The Ni films are covering the structure of the MCM-41. Also, Al particles could not be observed on the surface of the adsorbents [29]. Based on the last characterization results, it is possible to conclude that the whole set of materials revealed similar structural properties to the MCM-41 materials. Therefore, the differences observed in the adsorption experiments should not be only related to the structure of the MCM-41 and Ni/MCM-41, but also, the surface acidity plays an important role.

3.1.3. Temperature Programmed Desorption of Ammonia (NH$_3$-TPD) analysis

Considering the nitrogen physisorption, Fig. 4 illustrates the NH$_3$-TPD profiles normalized with the BET surface of the MCM-41 samples with different Si/Al ratio. As it has been reported in the open literature, MCM-41 is slightly acidic, but the Al incorporation increases strength and the number of acid sites [37-40]. The intensity of TPD profiles shows the total acidity of the adsorbents (Brönsted and Lewis acid sites). In Fig. 4, it can be observed that the surface density of the total acidity depends strongly on the Si/Al ratio. As can be observed, the sample without Al (SiAl = ∞) revealed a very low NH$_3$ adsorption and just a very broad desorption of low-intensity spectrum

13

could be observed. That means this sample presented the lowest acidity of all samples. The acidity of the rest of the samples increased considerably with the incorporation of Al and two broad desorption spectra could be recognized. The region of the spectra at low desorption temperature is associated with NH_3 desorption from weak Brönsted and Lewis acid sites and the NH_3 desorption at high temperature is associated with the presence of Brönsted and Lewis acid sites of medium strength [39,40]. It is also possible to recognize that the samples with a Si/Al ratio of 5 and 16 revealed the presence of the highest surface density of weak acid sites. The presence of this acidity might be due because of the higher amount of Al in these samples and because the difficulty of incorporating Al into the walls of the MCM-41, as it has been previously reported for the MCM-41 containing Ni at different Si/Al ratio [29]. These materials revealed a high surface acidity for two reasons: i) the Al incorporation and ii) the Ni incorporation [41]. On these last materials, the highest amount of Brönsted and Lewis acid sites was observed on Ni/MCM-41 increasing in the following order Si/Al ratio like: $\infty < 150 < 60 < 16 < 5$.

3.1.4. ^{29}Si and ^{27}Al Nuclear Magnetic Resonance (NMR) analysis

To investigate the Al incorporation into the walls of the MCM-41 materials, ^{29}Si CP-MAS NMR (Fig. 5a) and ^{27}Al MAS NMR (Fig. 5b) were carried out. In the first instance, the ^{29}Si CP-MAS NMR of the samples without Ni will be interpreted (Fig. 5a). For the case of the sample MCM-41, a very broad peak of very high intensity can be observed. This peak is centered at chemical shift of -100 ppm, which assigned to Q^3 units corresponding to a layer condensation of SiO_4 tetrahedral units. Around -93 ppm a shoulder of lower intensity could be recognized; this peak can be assigned to Q^2 units. Finally, there is an important contribution of Q^4 units observed at a chemical shift of around -118 ppm [42]. For the case of the Al MCM-41 containing samples, the intensity of all peaks was too much smaller than the corresponding samples with Ni [29]. All peaks are centered at -100 ppm, this peak is associated to the presence of structural unit's $Si(OSi)_3(OAl)$

in three-dimensionally connected aluminosilicate-like thermal-treated structures where Al is tetrahedral coordinated [43]. This broad peak might also be composed by $Si(OSi)_3OH$ units with also a very small contribution of $Si(OSi)_2(OAl)OH$ units [43]. The low intensity of the peaks for these samples might be due to the lack of ordering of the MCM-41 walls [43]. The intensity of these peaks is quite different from the samples containing Ni [29]. This strongly suggests that the Template Ion Exchange (TIE) improves considerably the degree of ordering the species present in the wall of the MCM-41. However, the species should be the same type in both samples. The Al incorporation into the MCM-41 walls was also investigated by ^{27}Al MAS NMR. From the Fig. 5b can be clearly seen that the incorporation of Al into the wall of the MCM-41 was quite successful for the case of the samples with a Si/Al ratio of 16, 60 and 150 (tetrahedral Al) because the adsorbents presented the higher acidity. This is concluded because the peak is mainly centered at 50 ppm [43]. For the sample with the highest Al content (Si/Al = 5) a very broad peak of high intensity can be recognized. This peak contains significant contributions of Al octahedral and Al pentahedral, according to the results reported [39,40]. The high intensity of the peak centered at 50 ppm might also be due to Al tetrahedral as extra-framework forming a condensate phase that has been reported in the literature for samples with low Si/Al ratio [44]. This condensate phase might trigger an essential modification of the nitrogen physisorption data because blocking of the pores (see Table 1). For the case of the Ni containing samples, very similar results have been obtained and published previously [29]. The most important difference is related to the intensity of the peaks. This might be due because of the TIE treatment for the incorporation of Ni, where it seems that promotes the improvement of the MCM-41 structure, this part will be considered as a further study.

Based on the characterization results, it was observed a significant difference in structure and acidic properties considering the varying of Si/Al ratio. Both aspects must be considered to explain the differences observed in the adsorption experiments with both sorbents.

15

3.2. Adsorption on MCM-41 and Ni/MCM-41 considering N and S compounds

Adsorptive denitrogenation and desulfurization of model fuel containing concentration of sulfur considering the DBT and nitrogen considering the Q, with N:S = 1 ratio, in dodecane as solvent at different initial concentrations (50-250 ppmw) over two adsorbents: MCM-41 (Fig. 6) and Ni/MCM-41 (Fig. 7) with Q in presence of DBT and varying the Si/Al ratio, are shown. The adsorption capacity of N when MCM-41 was used as an adsorbent in the presence of S at a low concentration of N like a 50-150 ppm and Si/Al = ∞ ratio was highest, moreover, when using Si/Al = 5 ratio has the lowest nitrogen adsorption are presented in Fig. 6a. The maximum adsorption of nitrogen was obtained by using the Si/Al = ∞ ratio because it presented a large surface area compared to the Si/Al ratio = 5 (see Table 1), although its ratio presented the lowest acidity. When increasing the initial nitrogen concentration content, the adsorption capacities decreased, this may due to the saturation of adsorbent. Additionally, sulfur removal is shown in Fig. 6b. Using MCM-41 with Si/Al = ∞ ratio was much lower than nitrogen removal approximately 10 times smaller (between 1-10 % of removal). The main difference was that at Si/Al = 5 ratio present the highest value at 50 ppmw of S and when increase the sulfur content, at high value ratio presented almost the same value although we have a smaller specific surface, by the results of NH_3-TPD and NMR analysis showed in characterization results (Section 3.1.3), we have more Lewis acid sites with this material and the DBT should be adsorbed in this sites, according to with Liao et al. [13] and Subhan and Liu [21]. Besides, when using Si/Al = 150 and ∞ ratio for all content of S presented the lowest values of removal between 1 and 3 %, this should be by diminishing of sites acid presumably Lewis.

On the other hand, the adsorption measurements of nitrogen removal as Q in the presence of sulfur as DBT in the model diesel fuel considering the Ni/MCM-41 as adsorbent and varying the Si/Al ratio are shown in Fig. 7. When using MCM-41 as adsorbent the behavior was very similar

16

than Ni/MCM-41 for removal of N using Si/Al=∞ ratio, however, for the other ratios it decreased

between 10 and 25%, it is because present almost the same specific surface, S_{BET}=930 m^2 g^{-1} with

MCM-41 (Table 1) and with Ni/MCM-41 using Si/Al = ∞ ratio the S_{BET}=1087 m^2 g^{-1} (Table 2),

just as the pore size presented same values, therefore the adsorption process is not influenced by

this parameter. [29]. Besides, when considering sulfur, as illustrated in Fig. 7b, we can see that at

low sulfur content the removal decreased. However, at high sulfur contents presented highest

removal at Si/Al = 5, it may be due to higher acidity in this material and that DBT is being adsorbed

on Ni particles, this is important, because the petroleum had higher content of sulfur, also reported

by García-Martínez et al. [31]. It should be noted that at high concentrations of nitrogen, the

adsorption was lower and that of sulfur was higher; this may be a problem because there is a higher

specific surface, pore diameter and pore volume available to adsorb the DBT (Table 1 and Table

2).

Thus far, the discussion of the results has been focused on the adsorption of nitrogen because

it seems that the mesoporous materials used are capable of adsorbing selectively Q from a mixture

of nitrogen and sulfur compounds on MCM-41 and Si/Al = ∞, and the adsorption capacity is much

higher than that of DBT. Therefore, the selective adsorption of nitrogen in the presence of sulfur

compounds becomes relevant to this kind of adsorbent. The high specific surface and wide pore

diameter of MCM-41 is one of the main factors in the adsorption of this basic molecule. On the

other hand, with Ni/MCM-41 at a low Si/Al ratio, the hypothesis that we have is the possibility

that acid Lewis sites are available on the surface of the mesoporous material at these temperatures

will function to adsorb the sulfur compound.

3.3. Adsorption kinetics

In this section shows the kinetic results, since the correlation coefficients were closed to the

unity in the same way that other works [27,28,31], the parameters calculated from kinetic models

are summarized in Table 3, the adsorption behavior of Q can be described appropriately by the pseudo-second-order kinetic in the same way that a lot of works [7,16,17,22,27,28,31,45]. Adsorption kinetics determine the adsorbate uptake rate of nitrogen and sulfur compounds. The adsorption kinetics of Q at different concentrations, expressed in parts per million weight of N in the presence of sulfur with DBT in model diesel fuel, are shown. The adsorption constant was adjusted with the linearized equation of the model (Eq. 4), considering the experimental data of the concentration of nitrogen in the form of Q. In Table 3, one may also note that the theoretical adsorption capacity expressed by the kinetic constant of adsorption (k_{ads}) and MCM-41 as adsorbent at the initial concentration of 50 ppmw of N presented the highest value of 25.7 g mmol^{-1} min^{-1} with Si/Al = 60 ratios followed by Si/Al = 16 and decreased when nitrogen content was increased (22-67 % at 100 ppmw) but when increasing the nitrogen content at 150 ppmw almost all remained constant, presenting an increase in the Si/Al = 60 and ∞, this may be due to the increase in surface area (Table 1). Moreover, when using the Ni/MCM-41, these values decreased than MCM-41 as adsorbent, but when using the Si/Al =16 at 250 ppmw of N this value (92.5 g mmol^{-1} min^{-1}) was higher than other values.

3.4. Isotherm adsorption using MCM-41 and Ni/MCM-41 with nitrogen using Q

These materials were used to remove Q and DBT molecules from model diesel fuel. In these experiments, it was shown that removal of nitrogen and sulfur atom were fitted to the corresponding isotherm, Langmuir or Freundlich models, and removal in the presence of both compounds at N:S = 1 ratio.

In Fig. 8 we can see the equilibrium adsorption against concentration at equilibrium results of nitrogen using Q with all ratio of Si/Al used in this work and both adsorbents: MCM-41: Fig. 8a and Ni/MCM-41: Fig. 8b, in both materials were higher values than reported by Silva et al. [46] that presented $q_e = 1.0$ mmol g $_{ads}^{-1}$ with Silica-Alumina as adsorbent. The dotted lines show the

18

adjustment of the isotherm to the experimental data; this adjustment was using the Langmuir isotherm for Si/Al = 150 and ∞ ratio and Freundlich isotherm for Si/Al = 5, 15 and 60 ratios with MCM-41 as adsorbent (Fig. 8a), presenting values higher (129 - 259 mg/g) than Ahmed et al. [47] between 110-170 mg/g. We can observe that the best fitting considering at Si/Al = 150 and ∞ ratio was when considering the Langmuir model, in the same way that Arcibar-Orozco et al. [48]. Thus, assume that Q adsorbs formation of a few adsorption layers, and it can be seen that the highest nitrogen adsorption was found at Si/Al = ∞ followed by 150 ratio. Besides, these should be by higher specific surface values with high Si/Al ratio (Table 1), moreover, with Si/Al = 5, 15 and 60 ratio the Freundlich model was adjusted at experimental data, this means that we have heterogeneous surface non-ideal and reversible adsorption, not restricted to the formation of monolayer. This empirical model can be applied to multilayer adsorption, with non-uniform distribution of adsorption heat and affinities over the heterogeneous surface [49]. For example, Chang Hyun et al. [50] used different materials in the adsorption of sulfur, these authors employed a beta zeolite (BEA), MCM-41 and SBA-15 with Ag as active phase, meanwhile the MCM-41 presented the higher surface area, no presented the better results in adsorption [50], but in the present work interesting results were found for the adsorption of both molecules. Furthermore, when using the Ni/MCM-41 as adsorbent (Fig. 8b) the maximum adsorption in Langmuir isotherm was lower than MCM-41 for almost all Si/Al ratio (30% approximately), because this empirical model assumes monolayer adsorption (the adsorbed layer is one molecule in thickness), with adsorption can only occur at a finite (fixed) number of definite localized sites, that are identical and equivalent, with no lateral interaction and steric hindrance between the adsorbed molecules, even on adjacent sites [51], except at Si/Al = 5 ratio, moreover the equilibrium concentration was higher with Ni/MCM-41 as adsorbent than MCM-41, shown in Fig. 8b.

19

Besides, in Table 4 are presented the values obtained from the constants for the theoretical model parameters using Langmuir and Freundlich isotherm and correlation factor that was adjusted considering the nitrogen adsorption with material MCM-41 and Ni/MCM-41 at N:S = 1 ratio. Considering MCM-41 as adsorbent (Table 4a) it is observed that the best model that fit high values of the correlation factor was that considering Langmuir (Si/Al = 150 and ∞), while the Freundlich model adjusted to small values of the Si/Al = 5, 16 and 60 ratios (Table 4b), this confirms what was found that there was a lower adsorption of the Q. We can see that at a low Si/Al ratio, the value of q_m showed the lowest values (between 1.65-1.75 mmol/g) and K_L presented values smaller than unity (0.63-1.57 L/mmol) between Si/Al = 5 - 60. However, when increasing the Si/Al ratio, the value of q_m and the constant of Langmuir K_L showed the values of 2.16 mmol/g and 19.09 L/mmol, respectively, at Si/Al = ∞ and the values of the other ratios were lower, these values are higher than reported by Arcibar-Orozco et al. [48] using carbon as adsorbent and Fe -Mn (q_m = 0.546 - 0.756 mmol/g and K_L=0.99-1.44 mmol/g). This helps us to confirm that Q is being adsorbed preferentially at high Si/Al ratio, it is worth mentioning that the correlation factor for low values of the Si/Al (5, 16 and 60) ratios were lesser than 0.98, moreover, with Si/Al (5, 16 and 60) ratios using the Freundlich isotherm the 1/n values were smaller than unity, this implies chemisorption's process and K_F increased the values in the same way that ratio (0.668-0.959 $L^{1/n}$ mmol$^{(n-1)/n}$/g). Besides, the values obtained from the constants for the isotherm that was adjusted considering the Q adsorption, but now with material Ni/MCM-41 was presented in Table 4, we can see in almost all values of the Si/Al ratio, the Langmuir model was adjusted. The Freundlich model was adjusted only with the Si/Al = 5 value, showing lower adsorption of the Q at this ratio, this means that we have heterogeneous surface, and possibly multilayer adsorption. At almost ratio of Si/Al the constant of Langmuir of q_m presented almost the same behavior that MCM-41 adsorbent (between 1.78 and 2.01 mmol/g), the above gives us serves to try to explain that Q is being adsorbed without

20

Ni. Moreover, the constant K_L presented values smaller than MCM-41 as adsorbent (between 0.26 - 5.37 L/mmol); this helps us to think that Q is being adsorbed preferentially and more quickly without Ni. Finally, in Table 4b shows the Freundlich parameters with MCM-41 and we can see that 1/n value is found between 0.011- 0.37, the Freundlich constant between 0.668-1.418 and correlation factor nearly to the unity between 0.964 and 0.987, considering low Si/Al ratio (5, 16 and 60). On the other hand, with Ni/MCM-41 only the low Si/Al = 5 was adjusted the correlation factor showing the following values of 1/n = 0.49 and $K_F = 0.470$ $L^{1/n}$ $mmol^{(n-1)/n}/g$, in the same way that MCM-41 with 1/n values implies chemisorption's process.

3.4. Isotherm adsorption with MCM-41 and Ni/MCM-41 with sulfur using as DBT

The adsorption removal with both sorbents was presented in Fig. 9, considering the sulfur as DBT with both adsorbents and N:S=1 ratio with MCM-41: Fig. 9a and Ni/MCM-41: Fig. 9a. The behavior present different forms that are shown with the Q and MCM-41 adsorbent (Fig 8). Since using Si/Al=5 and 16 show the highest removal for sulfur in the presence of nitrogen decreased when increasing the ratio for two adsorbents, meanwhile, with Si/Al > 60, shows lower sulfur adsorption, in the same way that Subhan et al. [45]. With the total sulfur capacity increase with the decline of Si/Al ratio and reaches to highest capacity of 12.5 mg S/g $_{ads}$ with Si/Al = 15 and DBT as precursor of S (518 ppmw S) with Ni, this revealed that the high sulfur capacity of sorbent correlated closely with high Lewis acid sites according with Subhan et al. [45] in pure case was between 1.8-11.1 mg/g. Moreover, these values are lower than reported by Arcibar-Orozco et al. [48], because the values are q_m = 0.136 - 0.155 mmol/g.

Results to describe the adsorption processes considering DBT indicate that the Langmuir model did not adjust to experimental data showing the values of factor correlation less than unity using two adsorbents (Table 5a and Table 5b). This is attributed to the fact that the amount of sulfur adsorbed in the adsorbent is tiny and that is why the model was not adequately adjusted to the

experimental data. According to density functional theory (DFT) used by Parr and Pearson [52] and Pearson's classification, DBT is considered a soft base and the ion Ni^{2+} are borderlines acids. When the ion of Ni^{2+} is loaded on the surface of MCM-41, the local hard acid of the surface is weakened, which enhances the adsorption of DBT. Furthermore, the π-complexation on the surface of Ni/MCM-41 also plays an essential role in DBT adsorption [53]. However, Freundlich model for two adsorbents is appropriate, which suggests that multilayer adsorption takes place for the adsorption of sulfur compound with MCM-41 (Table 5b), according with García-Martínez et al. [31], because they show that sulfur compound adsorb on Ni in Ni/MCM-41 adsorbent and involve π complexation on acid site possibly in acid Lewis sites.

Moreover, as can be seen with two adsorbents in Fig. 9 the DBT adsorption process is heterogeneous and infinite surface coverage of the adsorbate occurred without maximum adsorption. The value in Freundlich equation with MCM-41 of 1/n was found to be between 0.49 and 0.66 indicating various aspects like; nonlinearity degree of adsorption, possible chemical process. Moreover, when using Ni/MCM-41 as adsorbent the value in Freundlich equation of 1/n was found to be nearly and higher than the unity, indicating that the adsorption is a favorable process and multilayer adsorption, this indicates that saturation was not attained. Because the DBT is relatively poorly adsorbed, that is why there is no good fit of the model to the experimental data and therefore the decrease the adjust of experimental and theoretical data. Something important to consider is that Subhan et al. [45] revealing that Ni incorporation in AlKIT-6(15) can generate a large amount of acid sites in the sorbents necessary to carry out the adsorption of sulfur as DBT. Therefore, it can propose that the adsorption on DBT preferentially occurs on Ni in flat positions in the same way that García-Martínez et al. [31] and Colín-Luna et al. [54] and as discussed previously.

22

Moreover, the selectivity was calculated considering the Eq. (2), and the results were shown in Table 6 with both adsorbents: MCM-41 and Ni/MCM-41. We can see that using the MCM-41 as adsorbent; we can see that low content of N and Si/Al = ∞ shows the highest of selectivity value than the other concentrations of N and Si/Al ratio. Likewise, with Ni/MCM-41 as adsorbent the selectivity was lower than MCM-41, this means that MCM-41 presents more selectivity for eliminating the Q than Ni/MCM-41, but this lastly adsorbent is more selective for DBT adsorption.

4. Conclusions

Considering the characterization results, we observed that a higher Si/Al ratio showed the higher surface and at low Si/Al diminished the specific surface, and NH_3-TPD and NMR show that at Si/Al = 5 and 16 have higher acid sites than another Si/Al ratio. The modification successfully added small amounts of Ni that did not collapse the pore structure but increased the density of surface (acidic).

From the adsorption results with MCM-41 as adsorbent, the highest removal of N was at low concentration and high Si/Al ratio with both adsorbents, meanwhile, considering the S the highest removal was obtained at low Si/Al ratio (5 and 16), this means that the S removal capacity depended strongly on the acid sites. Regarding the Q adsorption the isotherm of Langmuir for Si/Al =150 and ∞ ratios assume the formation of a few adsorption layers and slightly acidic lowest acidity, at low Si/Al = 5, 16 and 60 ratio the Freundlich model was adjusted, thus we have heterogeneous surface non-ideal and reversible adsorption. Moreover, with the Freundlich isotherm was adjusted for the DBT, indicating that the adsorption is a favorable process and multilayer adsorption, with 1/n < 1 indicating nonlinearity degree of adsorption, possible chemical process.

On the other hand, when using the adsorbent Ni/MCM-41, almost all ratio the Langmuir model was adjusted, and the Freundlich model was adjusted only with the Si/Al = 5 value, showing lower adsorption of the Q. Moreover, the value $1/n \approx 1$ indicate that the adsorption is a favorable process and multilayer adsorption. The adsorption of Q over MCM-41 adsorbents at high Si/Al ratio is selective in comparison with Ni/MCM-41, but when considering DBT, the specific interactions between this molecule and metal ions involving acid-base interactions and π-complexation adsorption mechanism between S and metal ion, is the main factor enhancing the adsorption over Ni/MCM-41 at low Si/Al ratio. Besides, the adsorption kinetic can be illustrated by the pseudo-second-order model for both sorbents. Also, these materials were found to be found to be promising adsorbents for Q and DBT capture. Lastly, the selectivity MCM-41 with Si/Al = ∞ shows the highest (N/S) selectivity of 13,390 at 50 ppmw N compared to another Si/Al ratio, for example at 250 ppmw N. For future tests, the effect of sorbent regeneration on the performance of the system over multiple cycles should be investigated.

Acknowledgements

References

[1] G. W. Huber, A. Corma, Angew. Chem. Int. Ed. 46 (2007) 7184 - 7201.

[2] Y. M. Isa, E. T. Ganda, Ren. and Sust. Energy Rev. 81 (2018) 69 - 75.

[3] I. Naboulsi, B. Lebeau, C.F.L. Aponte, S. Brunet, M. Mallet, L. Michelin, M. Bonne, C. Carteret, J.-L. Blin, Appl. Catal. A: Gen. 563 (2018) 91 - 97.

[4] E. Ito, J.A. Rob van Veen, Catal. Today 116 (2006) 446 - 460.

[5] R. T. Yang, A. J. Hernández-Maldonado, F. H. Yang, Science 301 (2003) 79 - 80.

[6] A. Samokhvalov, B. J. Tatarchuk, Catal. Reviews: Sci. and Eng. 52 (2010) 381 - 410.

[7] G. C. Laredo, P. M. Vega-Merino, F. Trejo-Zárraga, Jesús Castillo, Fuel Process. Tech. 106 (2013) 21 - 32.

[8] J. H. Kim, X. Ma, A. Zhou, Ch. Song, Catal. Today 111 (2006) 74 - 83.

[9] Y. Shen, P. Li, X. Xub, H. Liu, RSC Adv. 2 (2012) 1700 - 1711.

[10] J. Rui, F. Liu, R. Wang, Y. Lu, X. Yang, Molecules 22 (2017), 305 - 317.

[11] Y. Zua, Y. Qina, X. Gaoc, H. Liuc, X. Zhanga, J. Zhanga, L. Song, Appl. Catal. B: Env. 203 (2017) 96 - 107.

[12] Z. Y. Zhang, T. B. Shi, C.Z. Jia, W. J. Ji, Y. Chen, M. Y. He, Applied Catalysis B: Env. 82 (2008) 1 - 10.

[13] J. Liao, Y. Zhang, L. Fan, L. Chang, W. Bao, Ind. Eng. Chem. Res. 58 (2019) 4572-4580.

[14] T. A. Saleh, K. O. Sulaiman, S. A. AL-Hammadi, H. Dafalla, G. I. Danmaliki, J. of Clean. Prod. 154 (2017) 401 - 412.

[15] M. Almarri, X. Ma, C. Song, Energy & Fuels 23 (2009) 3940 - 3947.

[16] S. K. Thaligari, V. Ch. Srivastava, B. Prasad, Clean Tech. Env. Policy 18 (2016) 1021 - 1030.

[17] D. Rameshraja, V. Ch. Srivastava, J. P. Kushwaha, I. D. Mall, Chem. Eng. J. 181 - 182 (2012) 343 - 351.

[18] J. A. Arcibar-Orozco, J. R. Rangel-Mendez, Chem. Eng. J. 230 (2013) 439 - 446.

[19] S. K. Thaligari, S. Gupta, V. Ch. Srivastava, B. Prasad, Indian J. of Ch. Tech. 25 (2018) 522 - 530.

[20] S. Jin, Q. Yue, T. Meng, H. Zhang, N. Jiang, M. Jin, R. Zhang, J. Porous Mater 24 (2017) 1697 - 1704.

[21] F. Subhan, B.S. Liu, Chem. Eng. J. 178 (2011) 69 – 77.

[22] S. Shahriar, X. Han, H. Lin, Y. Zheng, Int. J. Chem. React. Eng. 14 (4) (2016) 823 - 830.

[23] J. M. Palomino, D. T. Tran, J. L. Hauser, H. Dong, S. R. J. Oliver, J. Mater. Chem. A. 2 (2014) 14890 - 14895.

[24] J. L. Hauser, D. T. Tran, E. T. Conley, J. M. Saunders, K. C. Bustillo, S. R. J. Oliver, Chem. Mater. 28 (2016) 474 - 479.

[25] J. You, H. Song, J. Zhang, Ch. Chen, F. Han, Fuel 241 (2019) 997 - 1007.

[26] S. A. Shahriar, H. Lin, Y. Zheng, Ind. Eng. Chem. Res. 51 (2012) 14503 - 14510.

[27] J. C. García-Martínez, H. A. González Uribe, M. M. González-Brambila, J. A. Colín-Luna, Y. E. Escobedo-García, A. López-Gaona, L. Alvarado-Perea, Catal. Today 305 (2018) 40 - 48.

[28] J.C. García-Martínez, C.R. Tapia Medina, M.M. González-Brambila, A.K. Medina-Mendoza, J.A. Colín-Luna (2017), Int. J. of Chem. Reactor Eng. 2018; 20170238.

[29] L. Alvarado Perea, T. Wolff, P. Veit, L. Hilfert, F. T. Edelmann, C. Hamel, A. Seidel-Morgenstern, J. of Catalysis 305 (2013) 154 - 168.

[30] Yonemitsu M, Tanaka Y, Iwamoto M (1997) Chem. Mater. 9: 2679-2681.

[31] J. C. García-Martínez, H. A. González-Uribe, M. M. González-Brambila, N.G. Flores del Río, A. López-Gaona, L. Alvarado-Perea, J.A. Colín-Luna, Topics in Catalysis 61 (2018) 1721 - 1733.

[32] S. Azizian, R. N. Fallah, Appl. Surf. Sci. 256 (2010) 5153-5156.

[33] M. Songolzadeh, M. Soleimania, M. T. Ravanchi, Microporous and Mesoporous Materials 274 (2019) 54–60.

[34] C. T. Kresge, M. E. Leonowicz, W. J. Roth, J. C. Vartuli, J. S. Beck, Nature 359 (1992) 710 - 712.

[35] J. S. Beck, J. C. Vartuli, W. J. Roth, M. E. Leonowicz, C. T. Kresge, K. D. Schmitt, C. T. W. Chu, D. H. Olson, E. W. Sheppard, J. Am. Chem. Soc. 114 (27) (1992), 10834 - 10843.

[36] K. S. W. Sing, D. H. Everett, R. A. W. Haul, L. Moscou, R. A. Pierotti, J. Rouquerol, T. Siemieniewska, Pure Appl. Chem. 57 (4) (1985) 603 - 619.

[37] A. Corma, V. Fornes, M. T. Navarro, J. Perez-Pariente, J. Catal. 148 (2) (1994) 569 -574.

[38] M. Hartmann, A. Pöppl, L. Kevan, J. Phys. Chem. 100 (23) (1996) 9906 - 9910.

[39] H. Kosslick, G. Lischke, G. Walther, W. Storek, A. Martin, R. Fricke, Microporous Materials 9 (1–2) (1997) 13 - 33.

[40] H. Kosslick, G. Lischke, B. Parlitz, W. Storek, R. Fricke, Applied Catalysis A: General 184 (1) (1999) 49 - 60.

[41] T. Lehmann, T. Wolff, C. Hamel, P. Veit, B. Garke, A. Seidel-Morgenstern, Microporous Mesoporous Mater. 151 (2012), 113 - 125.

[42] M. Magi, E. Lippmaa, A. Samoson, G. Engelhardt, A. R. Grimmer, J. Phys. Chem. 88 (8) (1984) 1518 - 1522.

[43] G. Engelhardt, D. Michel, High-Resolution Solid-State NMR of Silicates and Zeolites, Page Bros., Norwich, Great Britain, 1987.

[44] K. R. Kloetstra, H. W. Zandbergen, H. Bekkum, Catal. Lett. 33 (1-2) (1995) 157 - 163.

[45] F. Subhan, Z. Yan, P. Peng, M. Ikram, S. Rehman, J. Hazardous Materials 270 (2014) 82 – 91.

[46] J.M.P.F. Silva, E.B. Silveira, A.L.H. Costa, C.O. Veloso, C.A. Henriques, F.M.Z. Zotin, M.L.L. Paredes, R.A. Reis, S.S.X. Chiaro, Ind. Eng. Chem. Res. 53 (2014) 16000 - 16014.

[47] I. Ahmed, M. Tong, J.W. Jun, C. Zhong, S.H. Jhung, J. Physical Chemistry C. 120 (2016) 407–415.

[48] J.A. Arcibar-Orozco, A.A. Acosta-Herrera, J.R. Rangel-Méndez, J. Cleaner Production 218 (2019) 69 – 82.

[49] A.W. Adamson, A.P. Gast, Physical Chemistry of Surfaces, sixth ed., Wiley-Interscience, New York, 1997.

[50] K. Chang Hyun, S. Hirn-Ill, P. Jong-Ho, H. Sang-Sup, K. Jong-Nam, Korean J. Chem. Eng. 24 (6) (2007) 1124-1127.

[51] K. Vijayaraghavan, T.V.N. Padmesh, K. Palanivelu, M. Velan, J. Hazard. Mater. B133 (2006) 304– 308.

[52] R.G. Parr, R.G. Pearson, J. Am. Chem. Soc. 105 (1983) 7512 – 7516.

[53] S. Velu, Ch. Song, M. H. Engelhard, Y.H. Chin, Ind. Eng. Chem. Res. 44(15) (2005) 5740-5749.

[54] J. A. Colín-Luna, G.E. Zamora-Rodea, A.K. Medina-Mendoza, L. Alvarado-Perea, C. Ángeles-Chávez, J. Escobar, J.G. Pacheco-Sosa, J. C. García-Martínez, Catal. Today. In Press.
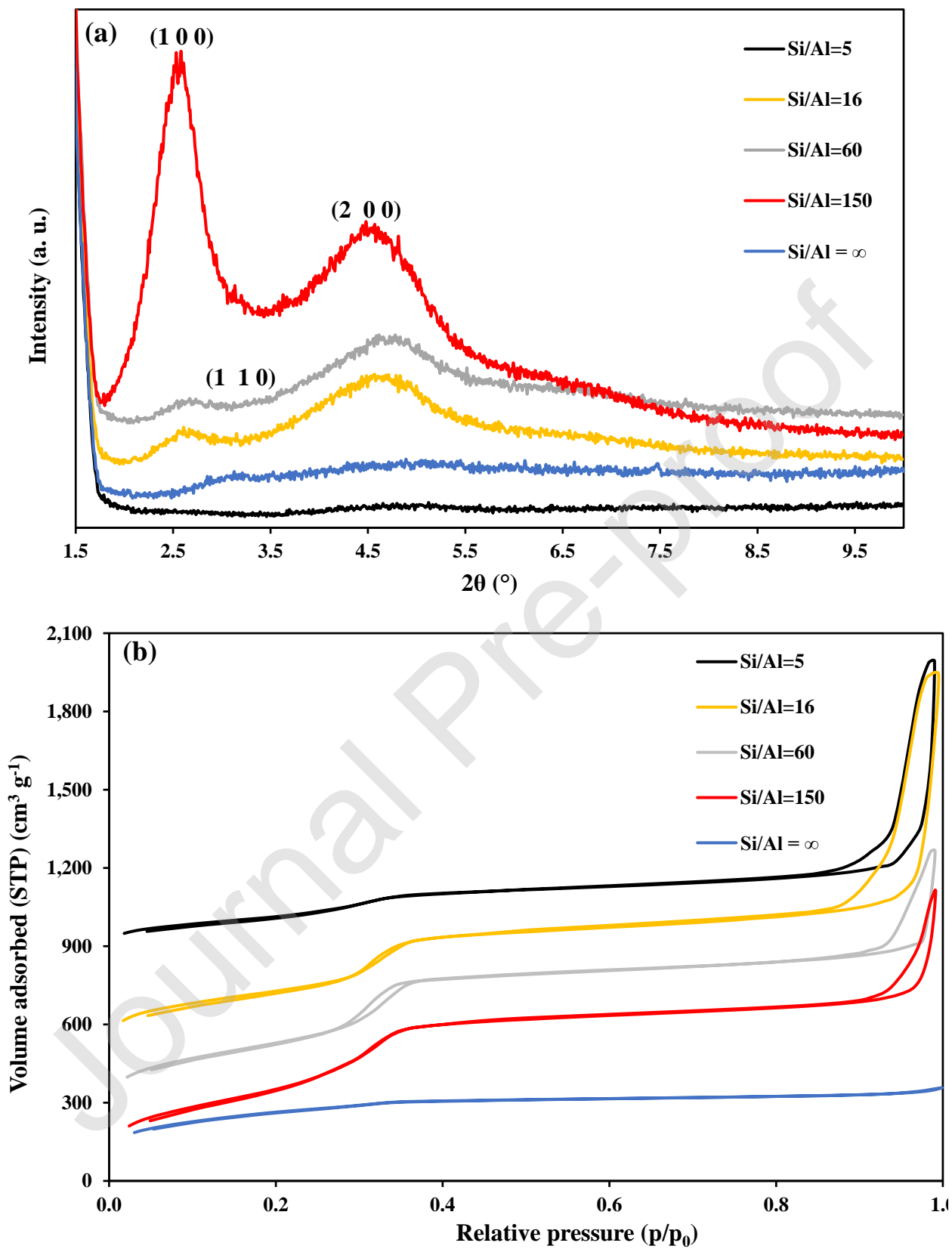
Fig. 1. (a) XRD patterns and (b) N$_2$-physisorption isotherms of MCM-41 at different Si/Al ratios.
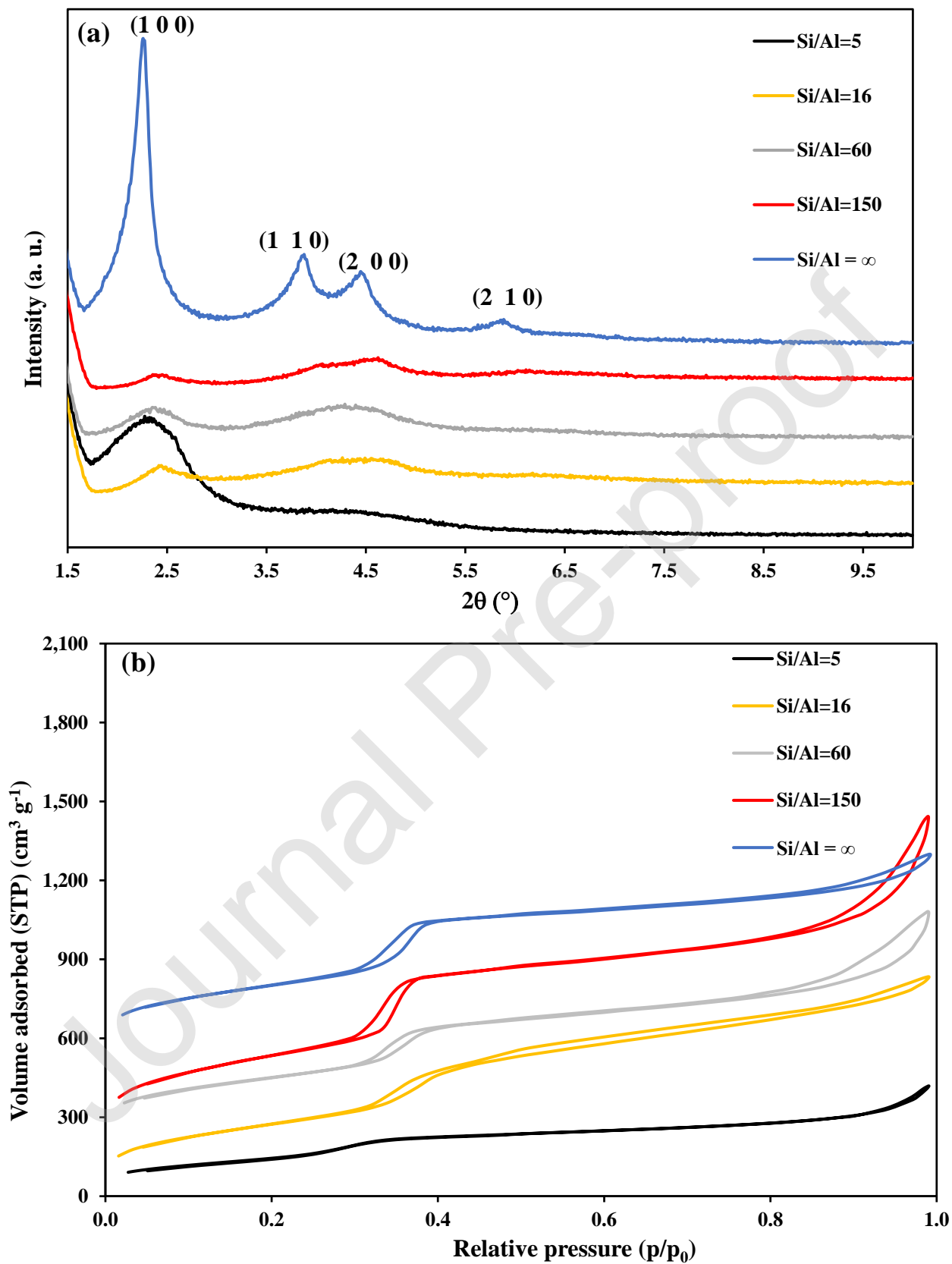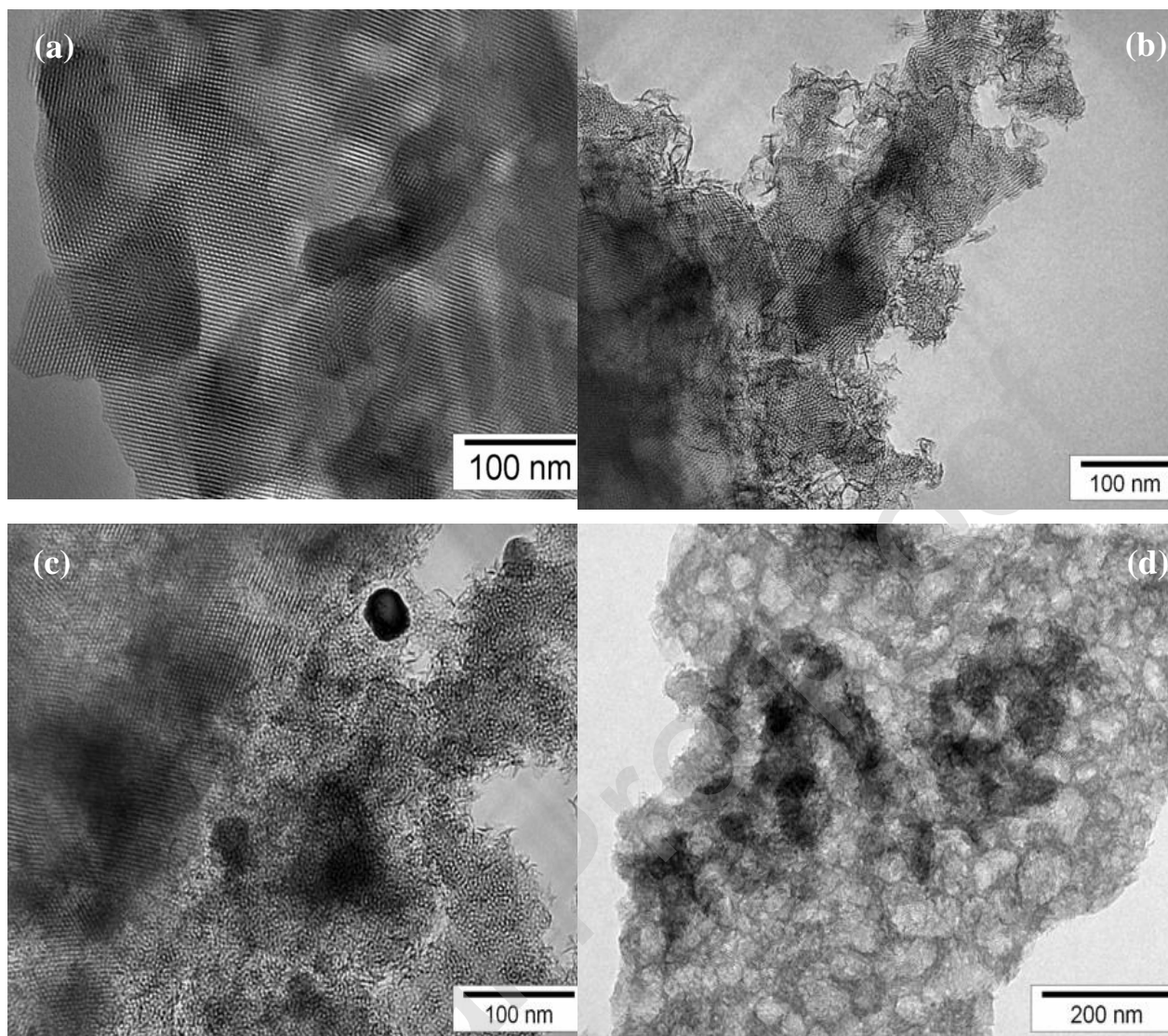
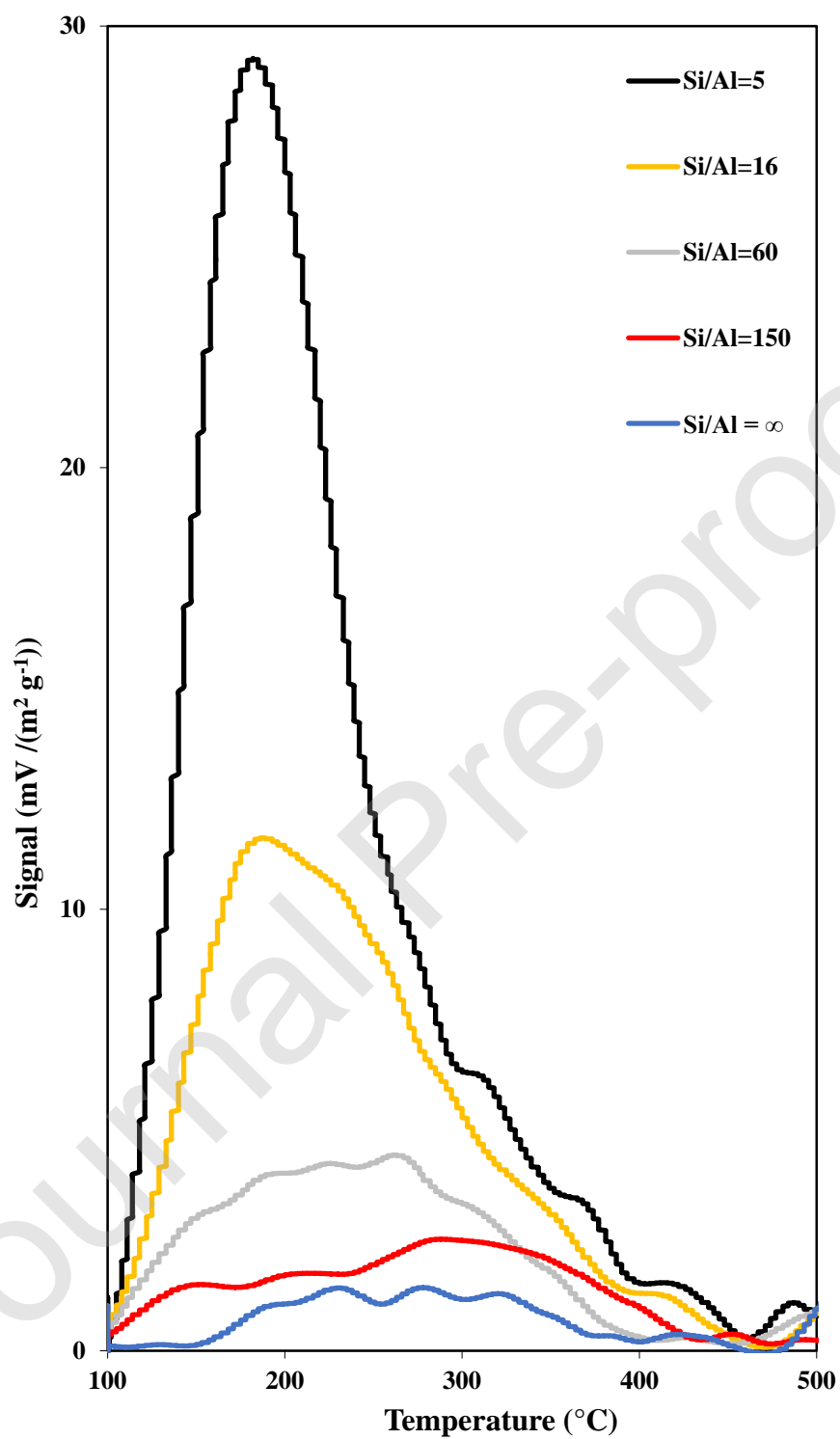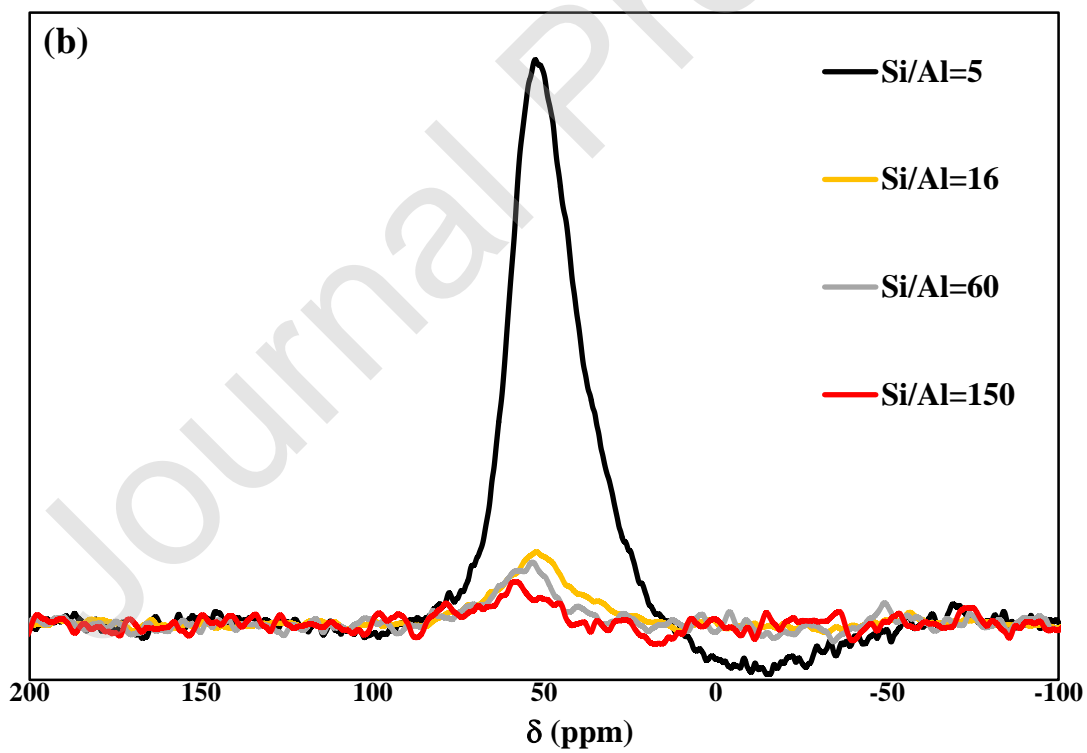**Fig. 2.** (a) XRD patterns and (b) N_2-physisorption isotherms of Ni/MCM-41 at different Si/Al ratios.

Fig. 3. TEM micrographs of (a) MCM-41, (b) Ni/MCM-41, (c) Ni/AlMCM-41 (Si/Al=150) and (d) Ni/AlMCM-41 (Si/Al=16).

Fig. 4. NH$_3$-TPD profiles of MCM-41 and AlMCM-41 as a function of the Si/Al ratio.
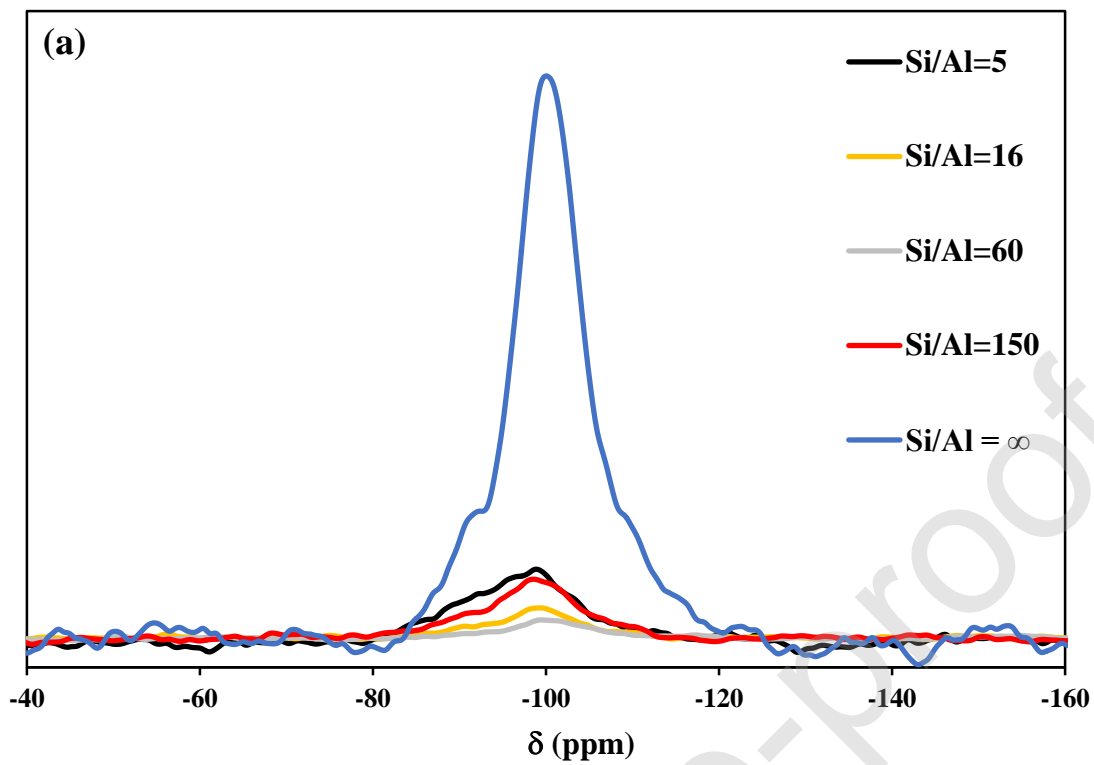
Fig. 5. (a) [29] Si CP-MAS NMR spectra and (b) [27] Al MAS NMR spectra indirect detection with MCM-41 at different Si/Al ratio.
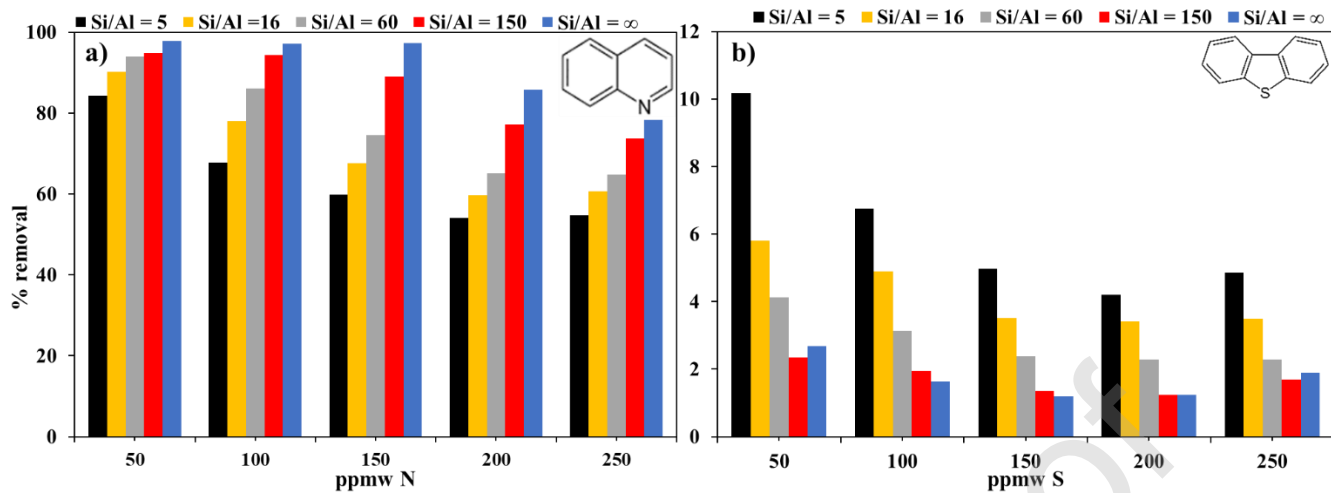
Fig. 6. a) Removal of N compound as a Q in the presence of S as DBT and b) removal of S compound in the presence of N on MCM-41 varying the Si/Al ratio, at different initial concentrations with a N:S=1 ratio at 313 K.
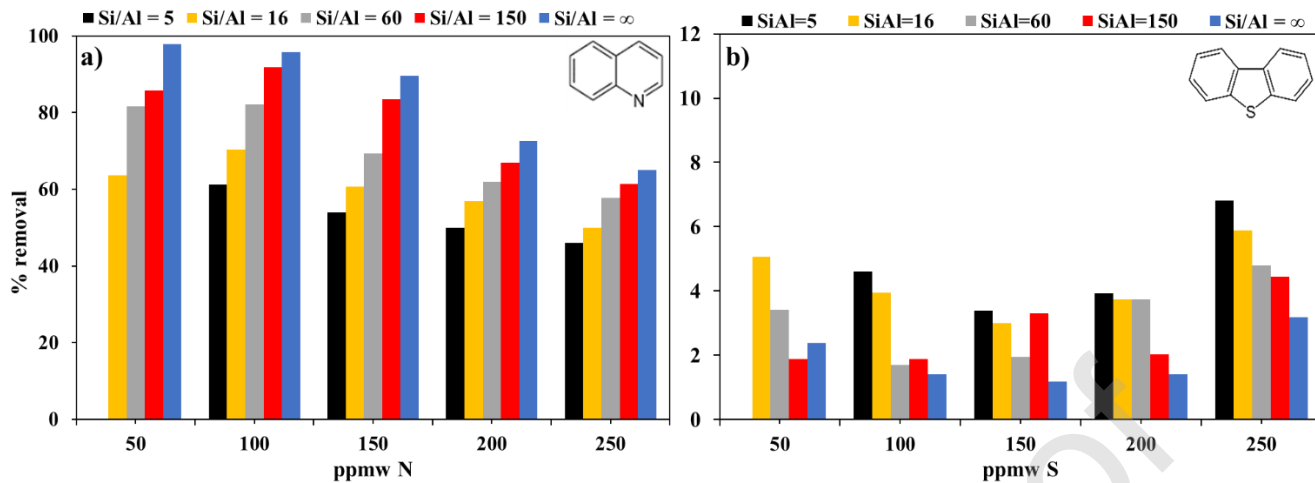
Fig. 7. a) Removal of N compound as a Q in the presence of S as DBT and b) S compound like DBT in the presence of N on Ni/MCM-41 varying the Si/Al ratio, at different initial concentrations with a N:S=1 ratio at 313 K.
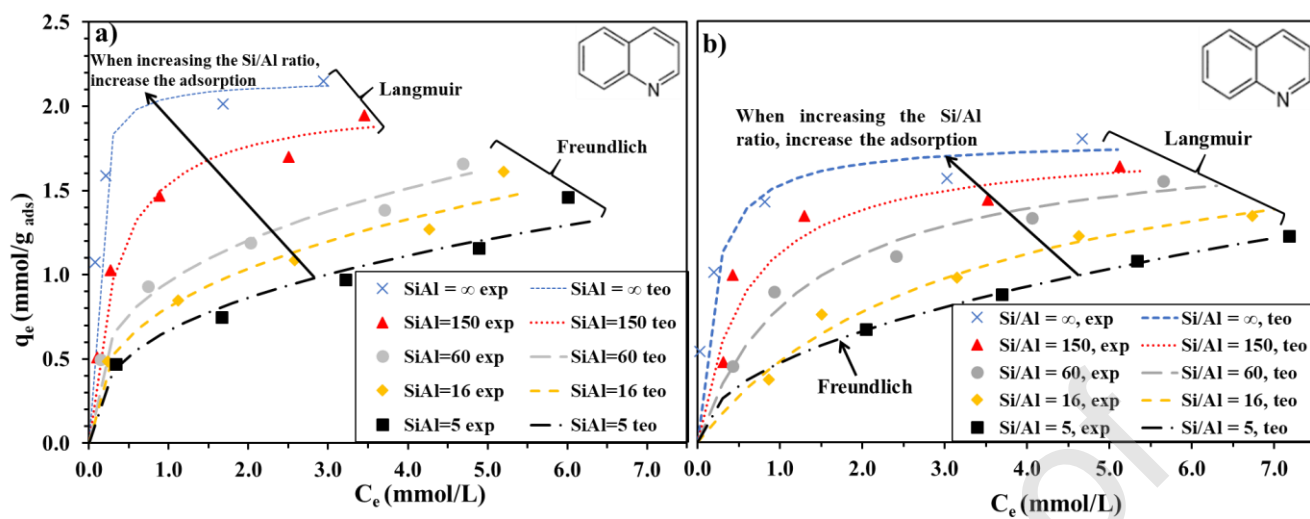
Fig. 8. Adsorption isotherms with a) MCM-41 and b) Ni/MCM-41 varying the Si/Al ratio with Q in the presence of DBT, with a N:S=1 ratio. Dashed lines represent Langmuir or Freundlich model.
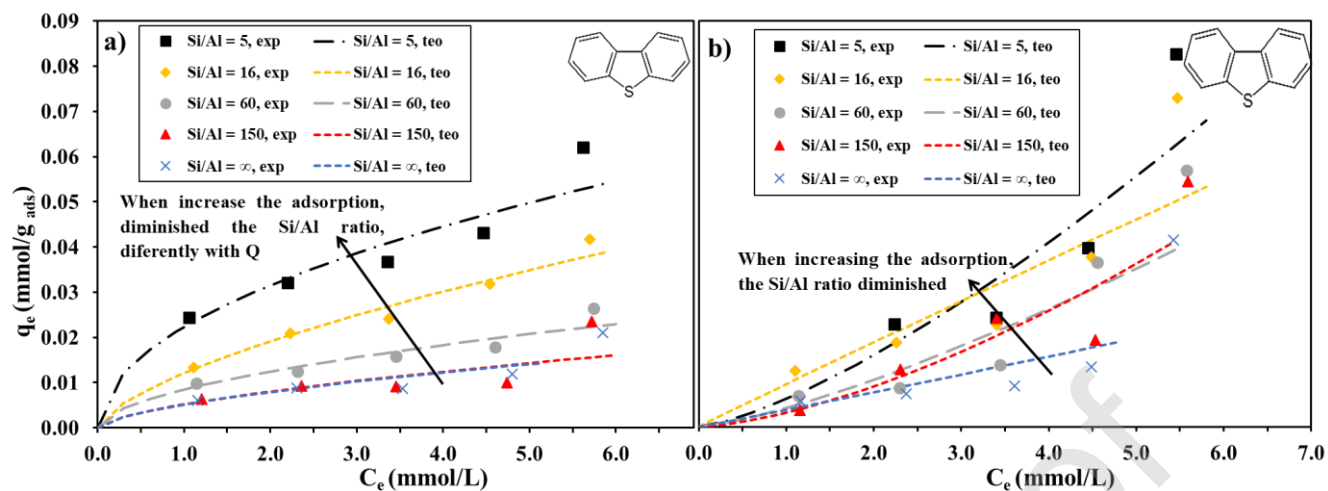
Fig. 9. Adsorption isotherms with a) MCM-41 and b) Ni/MCM-41 varying the Si/Al ratio with DBT in the presence of Q with a ratio N:S=1. Dashed lines represent the Freundlich model.

Table 1. N_2 physisorption results of MCM-41 at different Si/Al ratio.

Si/Al	BET specific surface ($m^2 g^{-1}$)	Pore Volume [1] ($cm^3 g^{-1}$)	Pore diameter BJH [2], (nm)
5	554	1.77	3.0
16	951	2.31	3.0
60	1095	1.65	3.0
150	1158	1.72	3.0
∞	930	0.55	3.0

[1] Pore volume at p/p_0=0.99.

[2] Pore diameter determined by Barret–Joyner–Halenda method (BJH) from the desorption branch.

Table 2. N_2 physisorption results of Ni/MCM-41 at different Si/Al ratio.

Si/Al	BET specific surface $(m^2\ g^{-1})$	Pore Volume [1] $(cm^3\ g^{-1})$	Pore diameter BJH [2], (nm)
5	533	0.6	3.0
16	928	1.3	3.0
60	919	1.4	3.0
150	1385	2.0	3.0
∞	1087	1.2	3.0

[1] Pore volume at p/p_0=0.99.

[2] Pore diameter determined by Barret–Joyner–Halenda method (BJH) from the desorption branch.

Table 3. Adsorption constants with MCM-41 and Ni/MCM-41 varying the Si/Al ratio at different concentrations of N and N/S = 1 ratio.

Ratio Si/Al	MCM-41 ppm N k_{ads} [g mmol^{-1} min^{-1}]					Ni/MCM-41 ppm N k_{ads} [g mmol^{-1} min^{-1}]				
	50	100	150	200	250	50	100	150	200	250
5	2.8	2.2	2.6	2.3	3.5	1.5	3.7	1.8	1.8	5.9
16	9.8	2.9	2.8	2.3	1.9	1.9	2.7	11.5	13.4	92.5
60	25.7	11.8	4.7	7.2	17.7	3.4	4.5	2.4	3.3	2.4
150	8.0	4.4	3.1	5.2	2.6	3.6	11.8	2.0	2.2	3.2
∞	3.4	1.9	4.2	9.3	9.8	3.1	10.6	5.3	36.1	0.9

Table 4. Theoretical model parameters for the adsorption of Q compounds varying the Si/Al ratio using both adsorbents: MCM-41 and Ni/MCM-41, a) Langmuir and b) Freundlich.

a)	MCM-41 Langmuir				Ni/MCM-41 Langmuir			
Ratio Si/Al	q_m (mmol/g)	K_L (L/mmol)	Equation	R^2	q_m (mmol/g)	K_L (L/mmol)	Equation	R^2
5	1.65	0.63	$q_e = \dfrac{1.04\,C_e}{1 + 0.63\,C_e}$	0.913	1.86	0.26	$q_e = \dfrac{0.48\,C_e}{1 + 0.26\,C_e}$	0.991
16	1.73	0.95	$q_e = \dfrac{1.64\,C_e}{1 + 0.95\,C_e}$	0.938	2.01	0.31	$q_e = \dfrac{0.62\,C_e}{1 + 0.31\,C_e}$	**0.956**
60	1.75	1.57	$q_e = \dfrac{2.75\,C_e}{1 + 1.57\,C_e}$	0.972	1.83	0.78	$q_e = \dfrac{1.43\,C_e}{1 + 0.78\,C_e}$	**0.983**
150	2.05	3.02	$q_e = \dfrac{6.19\,C_e}{1 + 3.02\,C_e}$	**0.993**	1.78	1.70	$q_e = \dfrac{3.03\,C_e}{1 + 1.70\,C_e}$	**0.986**
∞	2.16	19.09	$q_e = \dfrac{41.23\,C_e}{1 + 19.09\,C_e}$	**0.998**	1.80	5.37	$q_e = \dfrac{9.66\,C_e}{1 + 5.37\,C_e}$	**0.993**

b)	MCM-41 Freundlich				Ni/MCM-41 Freundlich			
Ratio Si/Al	1/n	K_F ($L^{1/n}$ mmol$^{(n-1)/n}$/g)	Equation	R^2	1/n	K_F ($L^{1/n}$ mmol$^{(n-1)/n}$/g)	Equation	R^2
5	0.37	0.668	$q_e = 0.668\,C_e^{0.37}$	**0.964**	0.49	0.470	$q_e = 0.470\,C_e^{0.487}$	**0.998**
16	0.36	0.808	$q_e = 0.808\,C_e^{0.36}$	**0.980**	0.59	0.481	$q_e = 0.481\,C_e^{0.59}$	0.919
60	0.33	0.959	$q_e = 0.959\,C_e^{0.33}$	**0.987**	0.43	0.753	$q_e = 0.753\,C_e^{0.43}$	0.932
150	0.35	1.340	$q_e = 1.340\,C_e^{0.35}$	0.914	0.35	0.999	$q_e = 0.999\,C_e^{0.35}$	0.741
∞	0.011	1.418	$q_e = 1.418\,C_e^{0.011}$	0.101	0.23	1.319	$q_e = 1.319\,C_e^{0.23}$	0.952

Table 5. Theoretical model parameters for the adsorption of DBT compounds varying the Si/Al ratio using both adsorbents: MCM-41 and Ni/MCM-41, a) Langmuir and b) Freundlich.

a)	**MCM-41 Langmuir**				**Ni/MCM-41 Langmuir**			
Ratio Si/Al	q_m (mmol/g)	K_L (L/mmol)	Equation	R^2	q_m (mmol/g)	K_L (L/mmol)	Equation	R^2
5	0.088	0.27	$q_e = \dfrac{0.024\,C_e}{1 + 0.273\,C_e}$	0.739	-0.090	-0.075	$q_e = \dfrac{0.0068\,C_e}{1 - 0.075\,C_e}$	0.245
16	0.081	0.15	$q_e = \dfrac{0.012\,C_e}{1 + 0.15\,C_e}$	0.747	-0.494	-0.017	$q_e = \dfrac{0.0085\,C_e}{1 - 0.017\,C_e}$	0.014
60	0.042	0.21	$q_e = \dfrac{0.009\,C_e}{1 + 0.21\,C_e}$	0.672	-0.042	-0.092	$q_e = \dfrac{0.0038\,C_e}{1 - 0.092\,C_e}$	0.320
150	0.036	0.14	$q_e = \dfrac{0.005\,C_e}{1 + 0.14\,C_e}$	0.220	-0.030	-0.108	$q_e = \dfrac{0.0032\,C_e}{1 - 0.108\,C_e}$	0.496
∞	0.036	0.135	$q_e = \dfrac{0.005\,C_e}{1 + 19.09\,C_e}$	0.302	-0.124	-0.026	$q_e = \dfrac{0.0033\,C_e}{1 - 0.026\,C_e}$	0.016

b)	**MCM-41 Freundlich**				**Ni/MCM-41 Freundlich**			
Ratio Si/Al	$1/n$	K_F ($L^{1/n}\,mmol^{(n-1)/n}/g$)	Equation	R^2	$1/n$	K_F ($L^{1/n}\,mmol^{(n-1)/n}/g$)	Equation	R^2
5	0.49	0.022	$q_e = 0.022\,C_e^{0.49}$	**0.898**	1.33	0.0062	$q_e = 0.0062\,C_e^{1.33}$	**0.772**
16	0.66	0.0121	$q_e = 0.0121\,C_e^{0.66}$	**0.969**	0.98	0.0095	$q_e = 0.0095\,C_e^{0.98}$	**0.837**
60	0.56	0.0084	$q_e = 0.0084\,C_e^{0.56}$	**0.932**	1.32	0.0042	$q_e = 0.0042\,C_e^{1.32}$	**0.824**
150	0.63	0.0052	$q_e = 0.0052\,C_e^{0.63}$	**0.652**	1.52	0.0031	$q_e = 0.0031\,C_e^{1.52}$	**0.913**
∞	0.63	0.0052	$q_e = 0.0052\,C_e^{0.63}$	**0.773**	1.03	0.0037	$q_e = 0.0037\,C_e^{1.031}$	**0.658**

Table 6. Selectivity with MCM-41 and Ni/MCM-41 varying the Si/Al ratio at different concentrations of N.

Ratio Si/Al	MCM-41 ppm N					Ni/MCM-41 ppm N				
	50	100	150	200	250	50	100	150	200	250
5	60	31	28	25	22	--	32	33	23	11
16	173	81	59	43	42	38	61	47	32	15
60	391	234	128	96	77	176	256	115	41	27
150	912	972	634	320	137	474	420	146	96	33
∞	13,390	3,623	3,028	488	203	3,500	1,627	695	175	51